Check for updates

Received: 5 January 2021 | Revised: 9 January 2022 | Accepted: 4 February 2022

DOI: 10.1002/hyp.14517

RESEARCH ARTICLE

WILEY

Comparing headwater stream thermal sensitivity across two distinct regions in Northern California

Austin D. Wissler | Catalina Segura | Kevin D. Bladon

Department of Forest Engineering, Resources, and Management, Oregon State University, Corvallis, Oregon, USA

Correspondence
Catalina Segura, 242 Peavy Forest Science Center, Corvallis, OR 97331, USA.
Email: segurac@oregonstate.edu

Funding information
California Board of Forestry and Fire Protection Effectiveness Monitoring Committee, Grant/Award Numbers: 8CA03650, 9CA04452

Abstract

Thermal regimes in headwater streams are critical for freshwater ecological condition and habitat resilience to disturbance, and to inform sustainable forest management. However, stream temperatures vary depending on characteristics of the stream, catchment, or region. To improve our knowledge of stream thermal regimes, we collected stream and air temperature data along eight headwater streams in two regions in Northern California. Five streams were in the Coast Range, which is characterized by permeable sandstone lithology, rain dominated precipitation regime, and dense coast redwood forests. Three streams were in the Cascade Range, which is characterized by fractured and resistant basalt lithology, snow dominated precipitation, and low to moderate density pine forests. We instrumented each stream with 12 stream temperature and four air temperature sensors during summer 2018. We compared stream thermal regimes and thermal sensitivity—slope of the linear regression between daily stream and air temperature—within and between study regions. Mean daily stream temperatures were ~4.7°C warmer in the Coast Range but were less variable (SD = 0.7°C) compared to the Cascade Range (SD = 2.3°C). Median thermal sensitivity was 0.33°C °C^{-1} in the Coast Range and 0.23°C °C^{-1} in the Cascade Range. We posit that the volcanic lithology underlying the Cascade streams likely supported discrete groundwater discharge locations of cold snowmelt water, which dampened thermal sensitivity. At locations of apparent groundwater discharge in these streams, median stream temperatures rapidly decreased by 2.0–7.0°C relative to locations 70–90 m upstream. In contrast, thin friable soils in the Coast Range likely contributed warmer, rain dominated baseflow from shallow subsurface sources, which strongly co-varied with air temperature and generally warmed downstream (up to 2.1°C km^{-1}). Our study revealed distinct longitudinal thermal regimes in streams with contrasting lithology, precipitation regimes, and stand densities suggesting that streams in these different regions may respond differentially to forest disturbances or climate change.

KEYWORDS
Caspar Creek, groundwater, headwater streams, lithology, thermal heterogeneity

 © 2022 John Wiley & Sons Ltd.

1 | INTRODUCTION

Stream temperature (T_s) is a critical water quality parameter that drives dissolved oxygen solubility (Loperfido et al., 2009; Ozaki et al., 2003), nutrient cycling (Morin et al., 1999; Neres-Lima et al., 2017), in-stream primary productivity (Bernhardt et al., 2018), and habitat provision (Armstrong et al., 2021; Bateman et al., 2021; Brewitt et al., 2017). When stream temperature warms, it can negatively impact sensitive cold water aquatic species, such as salmonid fishes and amphibians, by reducing habitat suitability for spawning and rearing life stages, and influencing individual metabolism and behaviour (Dallas & Ross-Gillespie, 2015; Eaton & Scheller, 1996; Hester & Doyle, 2011; McCullough et al., 2009; Sloat & Osterback, 2013; Welsh, Hodgson, Harvey, & Roche, 2001). Recent studies have illustrated that climate change and shifts in forest disturbance regimes have the potential to intensify thermal pollution and increase the risks to anadromous fish and other aquatic vertebrate populations (Benjamin, Connolly, Romine, & Perry, 2013; Jager et al., 2021; Thomas et al., 2004; Wagner et al., 2014) In Mediterranean climates, the threat to aquatic species is particularly important during the summer low flow period, when precipitation inputs are low and both thermal inputs from solar radiation and convective heat exchange between the warm air and cooler streams are at their maximum (Arismendi et al., 2013; Larsen & Woelfle-Erskine, 2018; Xu et al., 2010).

However, research on longitudinal thermal regimes of streams has revealed substantial complexity and variability in the dominant processes driving the spatial patterns in stream temperature (Fullerton et al., 2015; Fullerton et al., 2018; Hofmeister et al., 2015). For many years, the conventional perspective was that stream temperature increased progressively from headwaters to larger downstream river systems (Caissie, 2006; Vannote et al., 1980). Other studies have quantified decreasing stream temperature moving downstream in some headwaters (Dent et al., 2008; Leach & Moore, 2011; Moore, Sutherland, et al., 2005; Story et al., 2003) and larger streams (O'Sullivan et al., 2019). Additionally, recent advances in remote sensing technology and larger scale observations have revealed complex longitudinal profile patterns in stream temperature (Briggs et al., 2019; Dugdale et al., 2015; Ebersole et al., 2015). Similarly, technological developments in distributed fibre-optic measurements have illustrated the many opportunities that remain for quantifying and characterizing longitudinal stream thermal regimes (Ploum et al., 2018; Selker et al., 2006; Westhoff et al., 2011). This is especially true for non-fish bearing headwaters, where complex geomorphology and discrete groundwater inputs can produce distinct patterns of flow permanence and network connectivity (Gendaszek et al., 2020; Pate et al., 2020) that can influence stream temperature.

Despite recent advances in our knowledge, there is still much uncertainty about the longitudinal patterns in stream temperature due to numerous local and regional controls. One dominant local control on stream temperature is groundwater discharge, which in some systems can provide a stable supply of cool water and promote refugia for sensitive aquatic species during summer (Arscott et al., 2001; Briggs, Johnson, et al., 2018; Briggs, Lane, et al., 2018; Griebler & Avramov, 2015; Snyder et al., 2015). Groundwater contributions are, in part, controlled by regional lithology and are typically greater in more permeable geology (Hale & McDonnell, 2016). The magnitude of groundwater contributions may also be influenced by channel morphology (Johnson et al., 2014; Kasahara & Wondzell, 2003; Moore, Spittlehouse, & Story, 2005; Moore, Sutherland, et al., 2005; Story et al., 2003), direction of subsurface hydraulic gradients (Peterson & Sickbert, 2006), available alluvial hydraulic storage (Kelson & Wells, 1989), and catchment hydraulic conductivity (Morrice et al., 1997). In headwater streams, with a predominance of groundwater discharge and greater inputs of cold snowmelt, stream temperature is often cooler and less variable (Brown & Hannah, 2008; Danehy et al., 2010; Wagner et al., 2014). As such, stream segments with concentrated upwelling of groundwater can cause downstream cooling and reduce stream temperature variation, even during the winter (Moore, Spittlehouse, & Story, 2005; Moore, Sutherland, et al., 2005; Westhoff & Paukert, 2014). In such cases, streams with substantial groundwater discharge may be less responsive to reductions in canopy cover and subsequent increases in radiative loading (Bladon et al., 2016; Janisch et al., 2012; Larson et al., 2002) compared to streams with lesser groundwater contributions (Bladon et al., 2018; Dent et al., 2008; Moore, Spittlehouse, & Story, 2005). However, this may not always be the case as systems with shallow groundwater may be more sensitive to surface-subsurface energy exchange or other surface perturbations, leading to warming of subsurface water (Kurylyk et al., 2015).

Many empirical studies have used air temperature as a predictor of stream temperature and how stream temperature may respond to future climate change (Jackson et al., 2018; Kelleher et al., 2012; Mayer, 2012; Mohseni & Stefan, 1999; Segura et al., 2015; Snyder et al., 2015; Stefan & Preudhomme, 1993). Moreover, despite recent criticisms that the relationship between stream and air temperature often do not adequately characterize the underlying processes (Johnson, 2003; Leach & Moore, 2019), air temperature has been used successfully in some regions—including the Pacific Northwest, the Northeast, and Southeast US—to develop simple, empirical models of the relationship between stream temperature and warming air temperature due to climate change (Caldwell et al., 2015; Kelleher et al., 2012; Segura et al., 2015) or to identify locations of groundwater discharge (Fullerton et al., 2018; Mayer, 2012; Snyder et al., 2015). Air temperature has often been an effective predictor of stream temperature at coarse temporal scales (e.g., daily, weekly, monthly; Segura et al., 2015) and can act as a surrogate for total heat flux to the stream surface (Arismendi et al., 2014; Gomi et al., 2006; Gu et al., 2015; Tague et al., 2007).

The relationship between air and stream temperature is often described with a linear regression model in which the slope provides an indicator of the thermal sensitivity of the stream (Lisi et al., 2015; Segura et al., 2015; Snyder et al., 2015). This relationship can also be used as a proxy for stream-atmosphere energy exchanges and provide relatively inexpensive and rapid insights into the spatial extent of different streamflow contributions (Kelleher et al., 2012; Mayer, 2012).

For example, stream segments dominated by groundwater discharge or substantial hyporheic exchange may be identified by stable stream temperatures or lower thermal sensitivity to diel and seasonal variations in air temperature. Comparatively, stream segments with greater channelized flow or less groundwater or hyporheic contributions are likely to have stream temperatures that are more responsive to atmospheric energy exchanges. As a result, stream temperature and air temperature relationships have been used in many applications to assess contributions of groundwater and hyporheic flow (Briggs, Johnson, et al., 2018; Briggs, Lane, et al., 2018; Johnson et al., 2014; Selker et al., 2006; Snyder et al., 2015). However, the longitudinal variability in thermal sensitivity along headwater streams remains poorly characterized and the potential implications for headwater stream management in contrasting regions are not known.

In our study, we quantified both stream temperature and air temperature in eight headwater streams draining contrasting regions in Northern California. Specifically, we deployed 128 thermistors longitudinally down streams draining volcanic basalt (Cascade Range) and friable sandstone (Coast Range) lithology to characterize local and longitudinal trends in stream warming or cooling. We also sought to quantify the thermal sensitivity of streams, to provide insights into the regional differences in longitudinal stream-atmosphere energy exchanges and their influence on temperature variability in headwater streams. Thus, our primary objectives were to: (a) compare stream and air temperatures during the summer low flow period in streams draining contrasting regions, (b) quantify the reach-scale longitudinal variability in stream temperatures, and (c) quantify inter- and intra-regional thermal sensitivity. Our results revealed differences in the stream thermal regimes across our two study regions. We observed greater longitudinal thermal heterogeneity in streams underlain by basalt than sandstone, which we posit was driven primarily by the presence of discrete groundwater discharge locations that dominated over atmospheric control on stream temperature at these locations. This resulted in cooler average stream temperatures in the Cascade Range streams, despite warmer air temperatures and a less dense riparian canopy in this region.

2 | METHODS

2.1 | Study locations

Our study occurred in two distinct geological regions of Northern California: the Southern Cascade Range (LaTour Demonstration State Forest) and the North Coast Range (Caspar Creek Experimental Watershed in Jackson Demonstration State Forest) (Figure 1). The two regions were selected to represent strongly different climates, geologies, and dominant forest types (Table 1).

Our study included three streams in the Cascade Range: Beaver Creek, (BEA), Bullhock Creek (BUL), and Sugar Creek (SUG). All three streams are step-pool systems (Montgomery & Buffington, 1997) with few large cascades—they all have similar slope, canopy cover, and elevation (Table 2). Two of the streams had principally south-facing

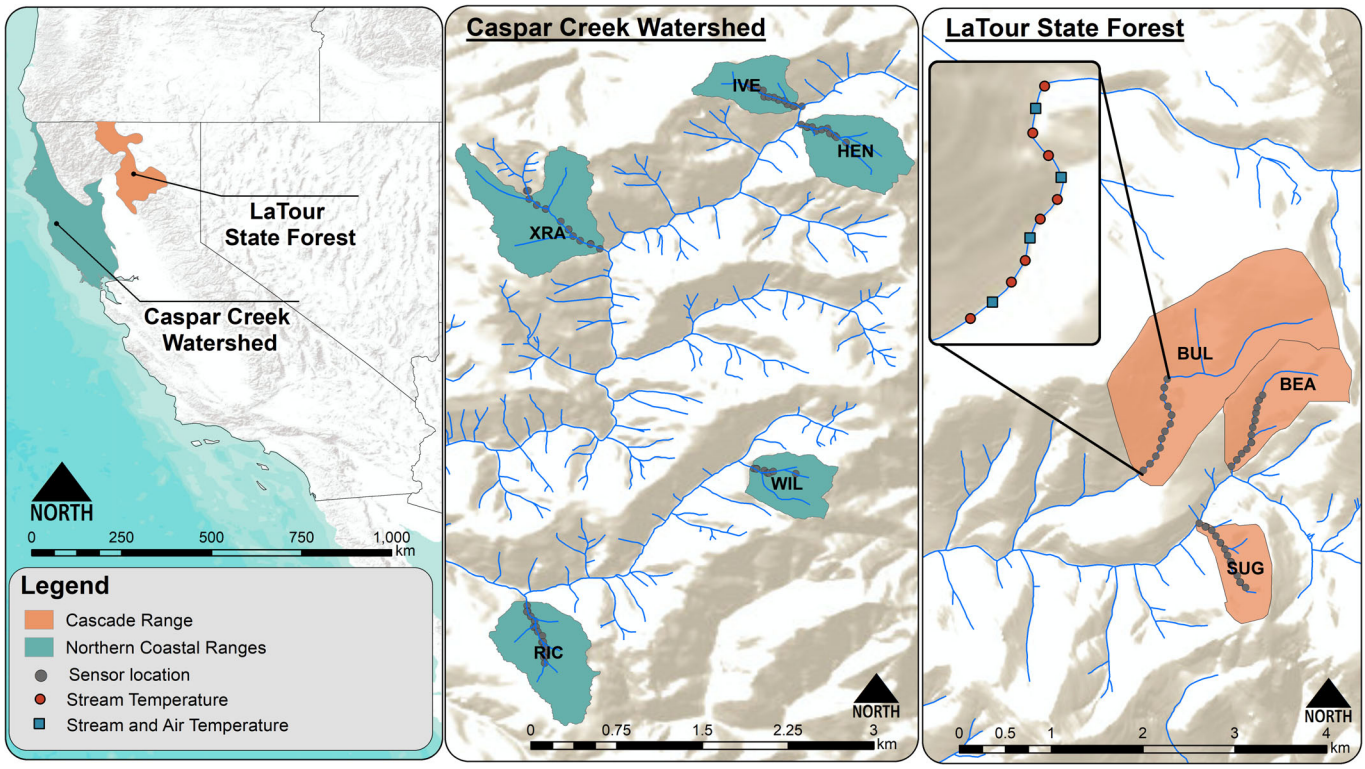

FIGURE 1 Field site locations within California in the LaTour State Forest (Cascade Range) and Caspar Creek (Coast Range). Inset on the right: Schematic of temperature data collection for all eight study reaches. Spacing between stream temperature sensors varied between streams and study regions (30–80 m)

TABLE 1 Climatic and physical characteristics of the study areas

Characteristic	Cascade Range	Coast Range	References
Mean T_a (°C, range)	10.9 (-6.0–29.2)	13.5 (1.6–28)	Measured herein
Precipitation (mm, Oct 2017–Sept 2018)	1018	956	PRISM Climate Group, 2020
30-year mean precipitation (mm)	1350	1262	PRISM Climate Group, 2020
Mean stream elevation (m, range)	1741 (1576–1912)	124 (52–189)	Measured herein
Mean watershed slope (%)	28	33	Measured herein
Mean canopy cover (%, range)	61 (54–66)	85 (78–91)	Oregon State LEMMA Database, 2020
Dominant forest cover	Sugar, ponderosa, and lodgepole pine	Coast redwood, Douglas-fir, and western hemlock	Observed herein
Dominant lithology	Andesite, basalt	Sandstone, mudstone	MacDonald, 1963; Amatya et al., 2016

aspects, while one stream was north-west facing. Soils are coarse, fast draining loams with depths <2 m (McDonald, 1995). The stream channel substrate was coarse gravel (D_{50}: 46–60 mm) except in locations behind debris jams where finer substrate accumulated (Pate et al., 2020). Valleys in the Cascade Range are U-shaped carved by glaciation processes with stream channels typically unconfined, except in some locations along Sugar Creek. The geology in the Cascade Range contains resistant, fractured basalt and andesite (Macdonald, 1963) characterized by rapid drainage to deep groundwater aquifers with long residence times (Tague et al., 2007; Tague et al., 2008) typical of volcanic geology (Jaeger et al., 2007). The climate is semi-arid, with hot, dry summers, and snowy, cold winters (CAL FIRE, 2008) (Table 1). Precipitation is snow dominated with snowpack persisting often into early May (PRISM Climate Group, 2020), with a snow water equivalent depth on April 1, 2018 of 384 mm (Snow Mountain, CA station, 18 km from study location; NRCS, 2020). The forests in our study catchments were dominated by 10 to 17 m tall sugar pine (*Pinus lambertiana*), lodgepole pine (*Pinus contorta*), and ponderosa pine (*Pinus ponderosa*), with some Douglas-fir (*Pseudotsuga menziesii*) and mountain hemlock (*Tsuga mertensiana*), with a comparatively low to moderate density canopy cover (LEMMA, 2020) (Table 1).

Study streams in the North Coast Range were located in the Caspar Creek Experimental Watershed Study, where research has been ongoing since 1961 addressing questions about forest management effects on forest hydrology and water quality (Cafferata & Reid, 2013; Keppeler et al., 1994). We included five streams in the Coast Range: Henningson (HEN), Iverson (IVE), Richards (RIC), Williams (WIL), and Xray (XRA) Creeks, which are step-pool systems (Montgomery & Buffington, 1997) with a few small cascades and similar slope, canopy cover, and elevation (Table 2); however, the streams all had slightly different aspects (Table 2). The channel substrate for all streams was medium gravel (D_{50}: 13–24 mm). Valleys are steep and V-shaped with considerable channel incision, resulting in strong confinement and coupling between the streams and hillslopes. Soils were 1 to 1.5 m deep, well drained loams underlain by a restrictive clay layer, which results in substantial pipeflow that rapidly transfers shallow subsurface flow laterally to the channel (Amatya et al., 2016; Keppeler & Brown, 1998). Geology of the region is dominated by friable sandstone and mudstone lithology of the Franciscan complex (Amatya et al., 2016). Winter climate is characterized as mild, cool, and wet, with temperatures rarely below 0°C, while summers are warm and dry (Keppeler et al., 1994) (Table 1). Precipitation is rain dominated, with >1200 mm falling annually (PRISM Climate Group, 2020). Riparian vegetation consists of 20 to 30 m tall, dense (canopy cover between 78 to 91%; LEMMA, 2020) coast redwood (*Sequoia sempervirens*) forest, with Douglas-fir (*Pseudotsuga menziesii*), grand fir (*Abies grandis*), and western hemlock (*Tsuga heterophylla*) occurring at lower densities (Cafferata & Reid, 2013).

2.2 | Data collection

In each of the eight study streams, we installed 16 HOBO TidbiT v2 sensors (Onset, Bourne, MA; accuracy ±0.21°C) between July 29 and

TABLE 2 Individual stream physical characteristics

	Cascade Range			Coast Range				
Characteristic	**BEA**	**BUL**	**SUG**	**HEN**	**IVE**	**RIC**	**WIL**	**XRA**
Mean stream slope (%)[a]	19	17	24	21	23	27	19	25
Stream length (m)	880	1078	902	418	418	550	308	770
Drainage area (km^2)[a]	1.07	3.13	0.58	0.38	0.23	0.47	0.26	0.62
Canopy cover (%)[b]	66	54	62	92	78	88	80	87
T_s sensor spacing (m)	73	90	75	35	35	45	25	64
D_{50} (mm)[c]	60	51	46	24	13	17	16	21
Stream aspect[a]	S	S	NW	W	SE	SW	NW	SE
Elevation range (m)[a]	1663–1777	1640–1772	1637–1837	104–155	104–164	52–110	135–189	71–178

[a]Derived using ArcMap version 10.7 (ESRI, Redlands, CA).
[b]Oregon State LEMMA Database (2020).
[c]From Pate et al. (2020).

August 1, 2017, to measure both air and stream temperature (128 total sensors). In this paper we analysed data recorded between June 1 and September 30, 2018 (122 days total) which correspond to the warmest stream temperatures typically recorded in the northern hemisphere (Dent et al., 2008; Groom et al., 2017). Specifically, we installed 12 stream temperature sensors and four air temperature sensors along each stream to collect continuous data (15-min intervals). The four air temperature sensors were co-located with stream temperature sensors near the top, bottom, and two midpoints of each stream (Figure 1, inset). The monitored stream length at each reach corresponded to the wet section—at the time of sensor installation in 2017—below the channel initiation point and upstream from the confluence with a higher order stream. Thus, while the monitored distance varied between reaches, all reaches were geomorphologically similar. Stream temperature sensors were regularly positioned approximately every 80 m in the Cascade Range reaches and every 30 to 60 m in the Coast Range reaches (Table 2, Figure 1). The sensors were placed along the thalweg and secured with rebar driven through the channel bottom. Air temperature sensors were placed adjacent to the channel and suspended from tree branches approximately 1 m above the ground. All sensors were enclosed in sections of white PVC tubing with drilled holes to allow fluid exchange and to minimize solar influences.

2.3 | Data analysis

Temperature data was first explored to remove periods when sensors were not submerged. To do this, we visually assessed and compared the diel temperature range of stream temperature and adjacent air temperature sensors to discern periods when sensors were dry (Campbell et al., 2013; Sowder & Steel, 2012). We discarded the data from 14 stream temperature sensors for our analysis because the sections of stream channels were dry over periods longer than 100 days. These sensors were located in both the Cascade region (two sensors) and the Coast Range region (12 sensors) (Table S1). One sensor, at XRA in the Coast Range, was lost and thus, the data was not included in the analysis (Table S1). Some of the remaining 81 stream temperature sensors went dry before the end of September 2018, resulting in time-series that varied in length between 18 and 122 days with most sites (56 out of 81) having >60 days of usable data (Table S1). If sensors were lost after being reported dry, we assumed the sensor remained dry throughout the remainder of the monitoring period (Arismendi et al., 2017). We did not make assumptions for sensors that were submerged prior to being lost. As a result, from the total possible stream temperature record (discarding dry periods) in the Cascade Range we were able to use 89% in SUG, 85% in BUL, and 94% in BEA. Comparatively, in the Coast Range we were able to use 72% of the possible data in HEN, 81% in IVE, 93% in WIL, 77% in XRA, and 83% in RIC (Figure S1). We note that the air temperature record was 89%–100% complete (Figure S2). Data exploration, quality control, and statistical analysis were conducted in R version 3.6.1 (R Core Team, 2020).

With the usable data, we quantified the diel range and daily maximum, minimum, median, and mean temperatures for each sensor, stream reach, and region. Statistically, we used one factor ANOVA with Tukey's post hoc tests to assess differences in daily mean air temperatures recorded among and within streams in both regions, and among streams in each region. Welch's two-sample *t*-test was used to assess differences in daily stream and air temperature metrics among regions.

2.3.1 | Assessing longitudinal stream temperature trends

We quantified the rate of downstream warming or cooling for each stream by fitting a linear regression equation with upstream distance (m) as the independent variable and average daily mean stream

temperatures at each sensor location (°C) as the dependent variable (-Figure S3). Regression slopes greater than zero indicated net downstream warming, while slopes less than zero indicated net downstream cooling.

We quantified the average incremental temperature difference (AITD) as the absolute value of the difference in the average mean daily stream temperatures between adjacent sensors within each individual stream. Specifically, we calculated AITD to provide an indicator of the site-level variability in stream temperature as:

$$\mathrm{AITD} = \frac{\sum_{i=1}^{n-1} |\mathrm{ADM}_i - \mathrm{ADM}_{i+1}|}{n-1} \quad (1)$$

where ADM_i was the average daily mean stream temperature measured at an upstream location, ADM_{i+1} was the average daily mean stream temperature measured at the nearest location downstream, and n was the number of stream temperature monitoring locations in each stream (8–12). Large values of AITD, were indicative of high variability in stream temperature magnitude from site to site. Alternatively, low values of AITD, were indicative of comparatively low site-level variability in stream temperature magnitude. Although the AITD metric captured variability in the central tendency of stream temperature at each monitoring location (average daily mean), it did not consider the variability in stream temperature at each monitoring location. For that reason, we also calculated the average incremental standard deviation difference (AISDD) as the absolute value of the difference between the average daily standard deviation in stream temperatures at each in-stream sensor and the one immediately downstream, using:

$$\mathrm{AISDD} = \frac{\sum_{i=1}^{n-1} |\mathrm{ADSD}_i - \mathrm{ADSD}_{i+1}|}{n-1} \quad (2)$$

where ADSD_i was the average of the standard deviation of daily stream temperature at an upstream location, ADSD_{i+1} was the average of the standard deviation of daily stream temperature at the location immediately downstream, and n was the number of stream temperature monitoring locations in each stream (8–12, Table S1). One value of AITD and AISDD was calculated for each stream to assess site-level thermal heterogeneity.

2.3.2 | Stream thermal sensitivity analysis

To assess relative differences in atmospheric control on stream temperature between and within streams in the Coast and Cascade Ranges, we used the linear relationship between mean daily stream and air temperatures (Equation (3)). Mean daily stream temperatures (T_s) for each in-stream sensor were regressed against mean daily air temperature (T_a) values from the nearest sensor as:

$$T_s = mT_a + b \quad (3)$$

where m is the regression slope (hence forth referred to as the thermal sensitivity) and b is the intercept. Thus, our analysis provided 8–12 linear regression equations per reach and corresponding thermal sensitivity values (considering the 15 discarded sites, Table S1). Prior to analysis, we removed air temperature data below 0°C as linear regression relationships between stream and air temperature were only valid for temperatures above freezing (Mayer, 2012; Morrill et al., 2005; Segura et al., 2015). Additionally, we also removed daily mean temperature values derived from less than a complete day of data (i.e., $n < 96$, 15-min interval data points) prior to fitting linear regression models—this resulted in removal of data from 23 days across all sites. Most regression equations (77 out of 81) between T_a and T_s were significant ($p < 0.05$, Figure S4). The four instances in which the correlation was weak were not included in the final analysis. We suspect that our methodology to discern dry periods was not accurate in these four cases (Figure S4). The coefficient of determination (R^2) was used to assess individual model fits. Median thermal sensitivity values measured in each region were compared using the non-parametric Wilcoxon Rank Sum test as it was determined that the distribution of thermal sensitivity values measured in the Cascade Range streams were not normally distributed (Shapiro–Wilk test, $p < 0.05$).

3 | RESULTS

3.1 | Summer air and stream temperatures

During summer 2018, mean daily air temperatures were 1.63°C (95% confidence interval [CI]: 1.49–1.75°C) warmer in the Cascade Range than in the Coast Range of California ($t = -24.67$, $p < 0.01$; Figure 2). Air temperatures were also more variable in the Cascade Range—the average diel air temperature range in the Cascade Range was ~2.3-times greater than in the Coast Range (Table 3). Daily maximum air temperatures in the Cascade Range (average: 26.2°C) were also greater than in the Coast Range (average: 17.6°C; $t = -74.52$, $p < 0.01$). Alternatively, daily minimum air temperatures were 1.45°C (95% CI: 1.33–1.59°C) warmer in the Coast Range (9.95°C) than in the Cascade Range (8.48°C; $t = 21.78$, $p < 0.01$).

There was strong evidence ($F_{2,2620} = 2.11$, $p < 0.01$) average daily mean air temperatures were different across streams within the Cascade Range (Figure 3). Comparatively, there was suggestive evidence ($F_{4,3399} = 2.11$, $p = 0.08$) that average daily mean air temperatures were different across streams within the Coast Range (Figure 3). However, there was strong evidence that both the average daily minimum ($F_{4,3399} = 16.64$, $p < 0.01$) and maximum ($F_{4,3399} = 89.73$, $p < 0.01$) air temperatures were different across streams in the Coast Range (Table S2). Longitudinally, the average daily mean air temperatures differed between proximate air temperature sensors in the Coast Range by 0.10–0.75°C and in the Cascade Range by 0.42–

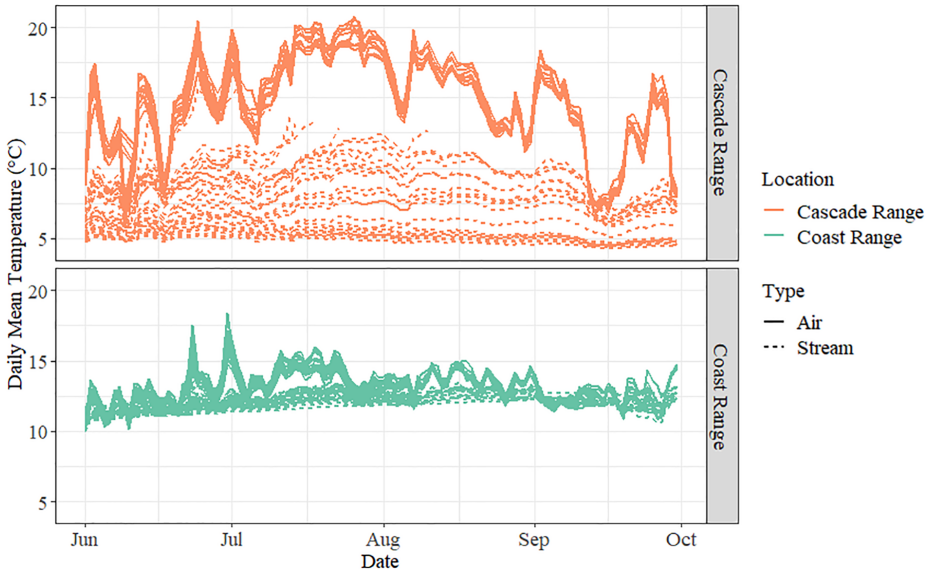

FIGURE 2 Time series of air (T_a) and stream (T_s) temperature data at all sites in the Cascade Range and Coast Range

TABLE 3 Stream (T_s) and air (T_a) temperature statistics during summer 2018 (June 1 to September 30) for streams in the Coast and Cascade Ranges

Type	Region	Avg. daily mean (°C)	Avg. daily SD (°C)	Avg. daily max (°C)	Avg. daily min (°C)	Avg. diel range (°C)
T_a	Cascade Range	14.73	5.48	26.22	8.49	17.73
	Coast Range	13.11	2.44	17.60	9.95	7.66
T_s	Cascade Range	7.30	0.68	8.77	6.53	2.24
	Coast Range	12.00	0.28	12.46	11.59	0.90

Abbreviations: Avg., average; SD, standard deviation.

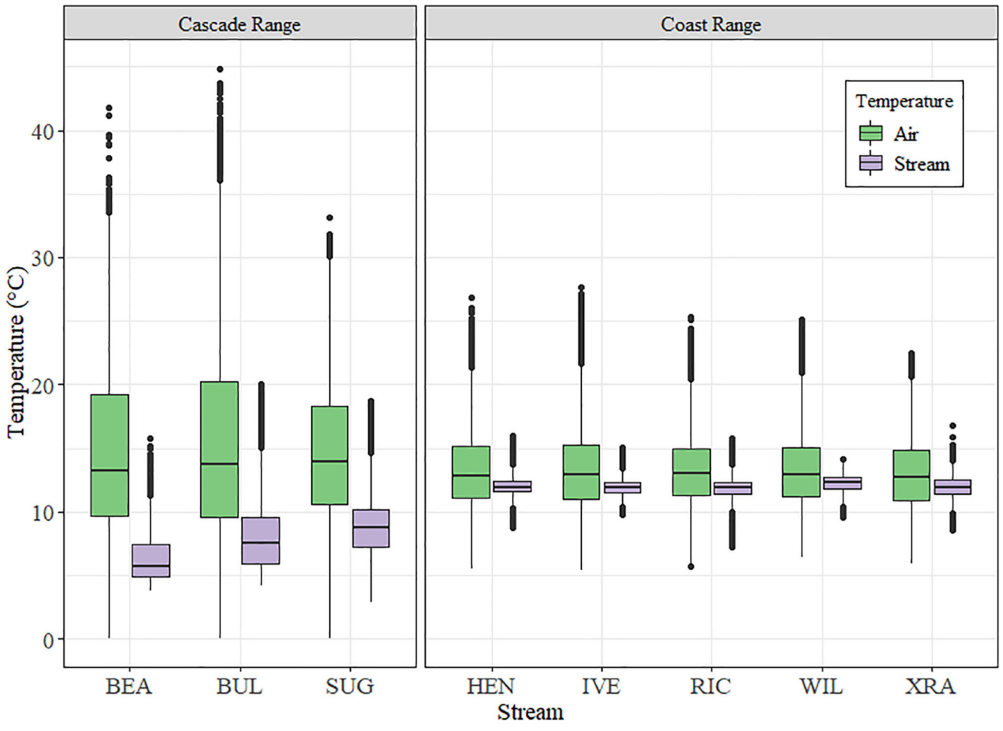

FIGURE 3 Comparison of air and stream temperature distributions among streams in the Coast and Cascade Ranges. Data were pooled from all temperature sensors within each stream. The boxplot central tendency line is the median, shaded boxes represent the interquartile range (IQR), whiskers represent the largest value up to 1.5-times the IQR, and the black dots indicate outliers beyond 1.5-times the IQR

2.2°C (Figure S3). Similarly, in the Coast Range the average daily minimum temperatures between proximate sensors varied by 0.08–1.45°C, while the maximum temperatures varied by 0.02–4.0°C. In the Cascade Range, the average daily minimum temperatures between proximate sensors varied by 0.10–2.95°C, while the maximum temperatures varied by 0.90–11.15°C.

The average daily mean stream temperature in the Cascade Range streams (7.3°C) was significantly cooler than in the Coast Range (12.0°C; $t = 112.4$, $p < 0.01$; Table 3). While the streams were cooler, the average diel stream temperature range in the Cascade Range (2.2°C day^{-1}) was ~2.5-times greater than in the Coast Range (0.9°C day^{-1}; $t = -45.79$, $p < 0.01$). We also found strong evidence average daily maximum stream temperatures in the Cascade Range streams (8.8°C) were cooler than in the Coast Range streams (12.5°C; $t = 72.3$, $p < 0.01$). Average daily minimum stream temperatures were also cooler in the Cascade Range streams (6.5°C) compared to the Coast Range streams (11.6°C, $t = 134.0$, $p < 0.01$). Site-level stream temperature statistics are available in Table S3.

3.2 | Longitudinal stream temperatures

Longitudinally down the length of our study streams in the Cascade Range, stream temperature generally cooled (−0.66 to −3.9°C km^{-1}) (Table 4). In contrast, four of the five streams in the Coast Range warmed (0.18 to 2.1°C km^{-1}) in the downstream direction, while HEN displayed moderate cooling (−1.1°C km^{-1}) (Figure 4). The average incremental temperature difference (AITD) between each stream temperature sensor and the one immediately downstream was greater in the Cascade streams (1.0°C) compared to the Coast Range streams (0.29°C; $t = 3.8$, $p = 0.03$), indicating greater longitudinal variability in stream temperature magnitude in the Cascade Range streams (Table 4). Despite these differences, we did not find statistical evidence that AISDD values were greater in Cascade Range streams compared to Coast Range streams ($t = 1.73$, $p = 0.11$; Table 4).

The three streams in the Cascade Range (underlain by volcanic lithology) exhibited substantial longitudinal variability in stream temperature (Figure 4). Overall, the site-level average daily standard deviation (SD) in stream temperature ranged from 0.19–1.84°C (mean = 0.68°C). Interestingly, we observed abrupt declines in average daily mean stream temperatures between two adjacent sensors of 2.0°C in SUG, 3.5°C in BEA, and 7.0°C in BUL (Figure 4). Stream temperatures generally warmed slightly between stream segments upstream from the locations of dramatic cooling. For example, the average daily mean summer stream temperature at BEA increased from 5.4 to 8.2°C between the first (furthest upstream sensor) and sixth temperature sensor (0.55 fractional distance upstream), which represented ~50% of the monitored distance (~400 m). However, the average daily mean summer stream temperatures abruptly decreased to 4.7°C (a loss of ~3.5°C) over the next ~80 m, between the sixth and seventh stream temperature sensors (between 0.55 and 0.45 fractional distance upstream) (Figure 4). We also noted that the variability in daily mean stream temperatures in BEA was generally greater (SD: 1.3°C) in the upper 400 m of the stream (i.e., above the segment where temperatures cooled rapidly), relative to the lower 480 to 880 m of stream (SD: 0.39°C). We observed similar patterns in summer stream temperatures in BUL and SUG, although both streams had ephemeral sections, which went dry during portions of the summer.

Comparatively, in the Coast Range, stream temperatures were more stable with no strongly discernible downstream warming or cooling trends (Figure 4). Site-level average daily standard deviations in stream temperature in the Coast Range ranged from 0.02 to 0.95°C (mean = 0.28°C). Generally, average daily mean stream temperatures increased moving downstream (Table 4), with the exception of the steam temperature at HEN, which cooled by 1.1°C km^{-1}. There were some sections of localized cooling and reduced stream temperature variability present in HEN, IVE, WIL, and XRA approximately mid-stream. For example, the average daily mean stream temperature decreased 0.67°C over 38 m between

TABLE 4 Longitudinal linear regression modelling results to assess downstream warming or cooling, and longitudinal heterogeneity in stream temperature in each stream

Region	Stream	Intercept (°C)	Slope (°C km^{-1})	AITD (°C)	AISDD (°C)
Cascade Range	BEA	5.08	−2.74	0.66	0.19
	BUL	6.15	−3.88	1.26	0.44
	SUG	8.42	−0.66	1.16	0.61
	Average	6.55	−2.43	1.03	0.41
Coast Range	HEN	11.79	−1.07	0.30	0.31
	IVE	11.93	0.18	0.21	0.15
	RIC	12.10	0.91	0.17	0.15
	WIL	12.42	2.12	0.36	0.21
	XRA	12.26	0.79	0.42	0.16
	Average	12.10	0.59	0.29	0.19

Abbreviations: AISDD, average difference in average daily stream temperature standard deviation between each stream temperature sensor and the sensor immediately downstream; AITD, average difference in average daily mean stream temperature between each stream temperature sensor and the sensor immediately downstream.

the fifth and sixth sensor location (from 0.64 to 0.55 fractional distance upstream) in HEN with a corresponding decrease in average daily standard deviation of stream temperature of 0.34°C (Figure 4). However, the largest change in average daily mean stream temperatures observed moving downstream between any two adjacent sites along the Coast Range streams was 0.91°C in XRA (between sensors 9 and 10, from 0.27 to 0.18 fractional distance upstream), which was 13% of the maximum change observed in the Cascade Range streams (Figure 4). The largest observed reductions in average daily mean stream temperature in the remaining three streams in the Coast Range were 0.31°C in IVE, 0.19°C in RIC, and 0.64°C in WIL (Figure 4).

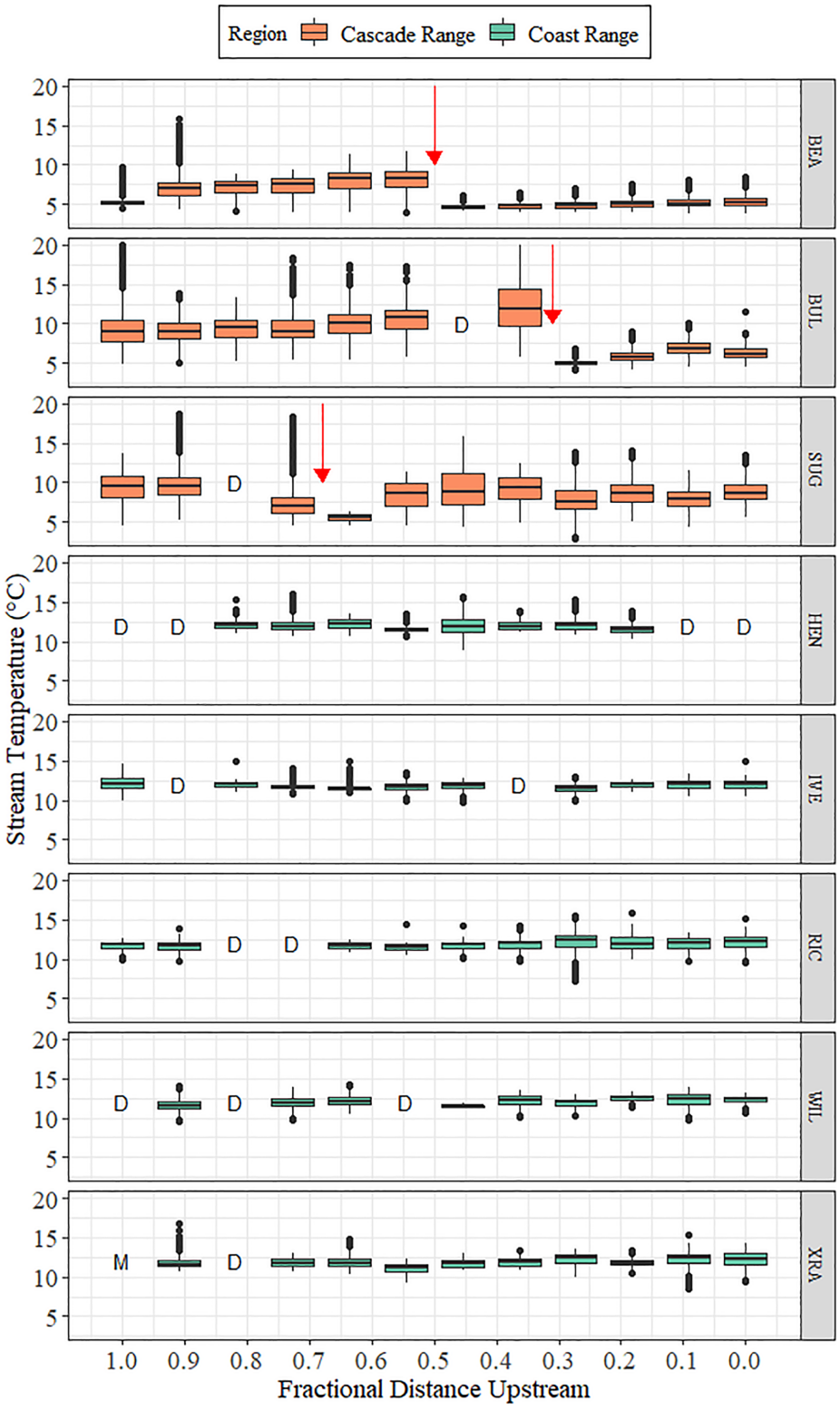

FIGURE 4 Longitudinal distribution of stream temperatures measured along Coast Range and Cascade Range streams during summer, 2018. Upstream distance is normalized on the *x*-axis for comparison. The direction of flow is from left to right. Red arrows indicate likely spring locations in the Cascade Streams. Locations shown without data were either dry (D) throughout the summer or the sensor was missing during data collection (M). Measured stream lengths vary from 300 to 1000 m

3.3 | Stream thermal sensitivity

Our site-level linear regression models between air and stream temperature revealed fine-scale spatial variability in stream thermal sensitivity to air temperature in both study regions (Figure 5). In the Cascade Range streams, the median site-level thermal sensitivity was 0.23°C °C^{-1}, ranging between 0.04–0.63°C °C^{-1} (R^2 = 0.11–0.85) (Table 5). Interestingly, in BUL, the thermal sensitivity increased consistently from 0.27°C °C^{-1} at the uppermost sensor to a maximum of 0.63°C °C^{-1} at the eighth sensor (0.36 fractional distance upstream). However, the thermal sensitivity dramatically decreased to 0.04°C °C^{-1} at the next sensor downstream and stream temperature generally remained decoupled from air temperature across the bottom ~20% (starting at 0.27 fractional distance upstream) of the stream reach (Figure 5).

Similarly, in BEA the thermal sensitivity increased from 0.05°C °C^{-1} at the uppermost sensor to 0.31°C °C^{-1} at the sixth sensor (0.55 fractional distance upstream), before also decreasing dramatically to 0.06°C °C^{-1} at the seventh sensor (0.45 fractional distance upstream) (Figure 5). The stream temperature in BEA also generally remained decoupled from air temperature for the remainder of the monitored stream length, which was similar to BUL.

In SUG, site-level thermal sensitivity decreased from 0.32°C °C^{-1} to 0.10°C °C^{-1} over the first 328 m (to 0.64 fractional distance upstream). Thermal sensitivity in SUG then increased from 0.10°C °C^{-1} to 0.59°C °C^{-1} over 150 m from the fifth to sixth sensor (from 0.64 to 0.45 fractional distance upstream) before alternately decreasing to 0.28°C °C^{-1} at 0.27 fractional distance upstream then increasing to 0.45°C °C^{-1} at 0.18 fractional distance upstream.

Despite the variability in thermal sensitivity in the Cascade Range, the distribution of thermal sensitivity values was skewed to values less than 0.2 (Figure 6a), and these locations generally had the coolest stream temperatures. For instance, across the three Cascade Range streams, there was a strong, positive linear relationship between site-level thermal sensitivity values and the average daily mean stream temperature (R^2 = 0.79). Positive relationships also existed between site-level thermal sensitivities and average daily maximum stream temperatures (R^2 = 0.63), and average diel stream temperature range (R^2 = 0.59) (Figure S5). In other words, warmer stream segments were generally more coupled to air temperature, while cooler stream segments were less coupled with air temperature.

In the Coast Range, the median site-level thermal sensitivity was 0.33°C °C^{-1} and ranged between 0.10–0.77°C °C^{-1} (R^2 = 0.11–0.93) (Table 5). Statistically, the median thermal sensitivity in the Coast Range was greater than in the Cascade Range streams (Wilcoxon Rank Sum test, p < 0.01, 95% CI: 0.039–0.171) (Table 5). Longitudinal patterns in thermal sensitivity varied by stream, but generally increased moving downstream in RIC and XRA (Figure 5). For instance, thermal sensitivity increased from 0.20 to 0.53°C °C^{-1} over 300 m from mid-reach (0.55 fractional distance upstream) to the bottom of RIC and from 0.26 to 0.49°C °C^{-1} over 210 m in XRA (from 0.27 fractional distance upstream to the bottom of XRA). Alternatively, longitudinal trends in thermal sensitivity for streams HEN, IVE, and WIL did not show strong increasing or decreasing trends. However, there were some stream segments in those three streams where thermal sensitivity between proximate temperature sensors changed rapidly. For instance, in WIL the thermal sensitivity

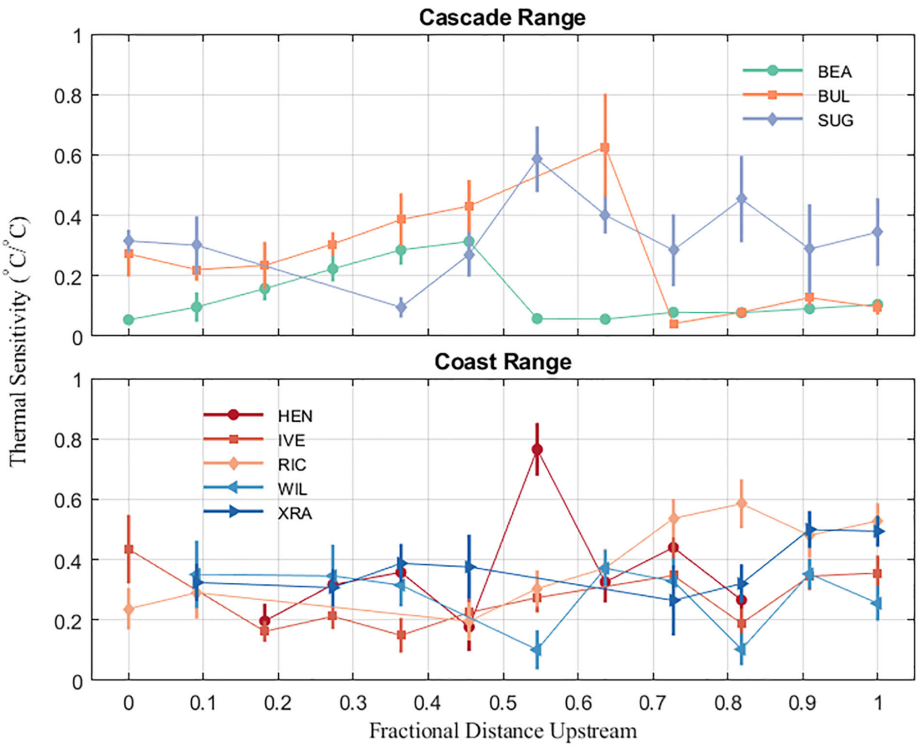

FIGURE 5 Longitudinal trends in thermal sensitivity (linear regression slope, Equation (3)) along Cascade Range (BEA, BUL, SUG) and Coast Range (HEN, IVE, RIC, WIL, XRA) streams. The error bars correspond to the 95% confidence intervals. Missing data points indicate sensors that went dry or regression models that were not included in the final analysis. The largest value in HEN is characterized by a sensor that went dry after 17 days. The *x*-axis is normalized for ease of comparison; stream lengths are in Table 2. The 95% confidence intervals may be slightly underestimated due to the potential autocorrelation in the data

TABLE 5 Thermal sensitivity descriptive statistics for each stream and region

Region	Stream	# of T_s sensors	Mean R^2 (range)	Mean (°C °C^{-1})	Median (°C °C^{-1})	SD (°C °C^{-1})	Minimum (°C °C^{-1})	Maximum (°C °C^{-1})
Cascade Range	BEA	12	0.55 (0.11–0.85)	0.13	0.09	0.09	0.05	0.31
	BUL	11	0.64 (0.48–0.84)	0.26	0.23	0.18	0.04	0.63
	SUG	10	0.55 (0.30–0.71)	0.33	0.31	0.13	0.10	0.59
	Sub-totals	33	0.58 (0.11–0.85)	0.24	0.23	0.16	0.04	0.63
Coast Range	HEN	8	0.60 (0.44–0.93)	0.36	0.32	0.19	0.18	0.77
	IVE	10	0.60 (0.32–0.78)	0.27	0.25	0.10	0.15	0.44
	RIC	9	0.55 (0.28–0.75)	0.39	0.37	0.14	0.20	0.59
	WIL	9	0.48 (0.11–0.65)	0.28	0.33	0.11	0.10	0.37
	XRA	8	0.66 (0.35–0.78)	0.37	0.35	0.09	0.27	0.50
	Sub-totals	44	0.58 (0.11–0.93)	0.33	0.33	0.13	0.10	0.77

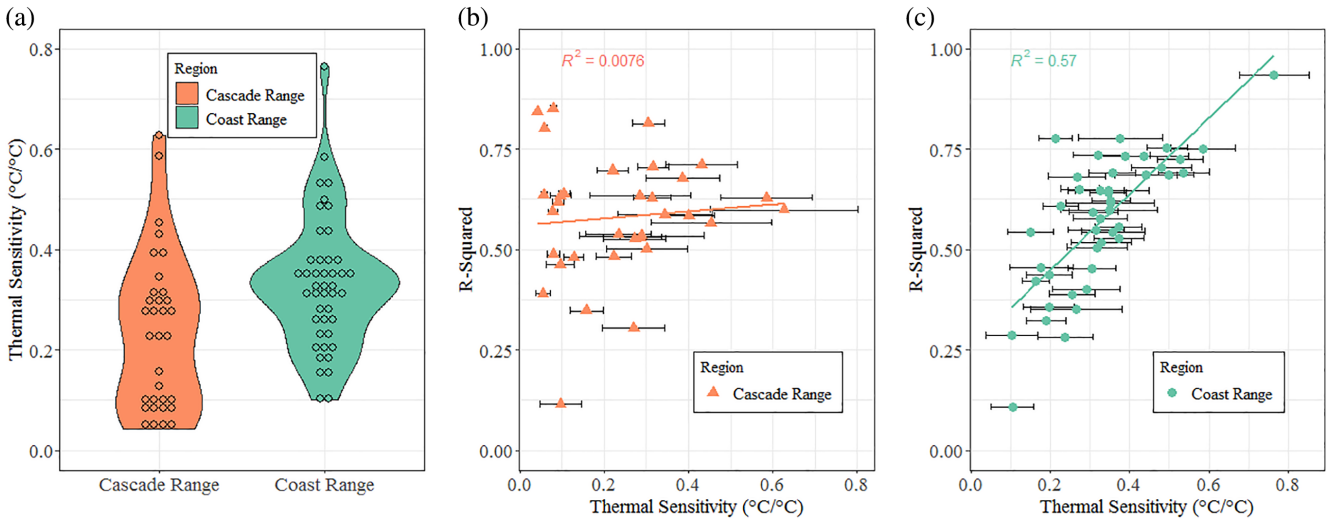

FIGURE 6 (a) Violin plot showing the distribution of thermal sensitivities of streams in the Cascade Range and the Coast Range. The relationship between site-level thermal sensitivity values and model R^2 values is also shown for (b) Cascade Range sites and (c) Coast Range sites. Error bars in panels (b) and (c) denote the 95% confidence intervals

increased from 0.10 to 0.37°C °C^{-1} over 28 m (from 0.45 to 0.36 fractional distance upstream), then decreased again to 0.10°C °C^{-1} over 56 m moving downstream starting at 0.18 fractional distance upstream. The largest change in thermal sensitivity observed in the Coast Range streams occurred mid-reach (0.45 fractional distance upstream) in HEN, where thermal sensitivity increased from 0.18 to 0.77°C °C^{-1} over 38 m and then decreased to 0.33°C °C^{-1}; however, this stream segment went dry 17 days after the start of monitoring (June 18, 2018). Contrary to results in the Cascade Range, variability in site-level thermal sensitivity values in Coast Range streams was not well explained by the average daily mean stream temperature (R^2 = 0.06), indicating that the most thermally insensitive locations along Coast Range streams were not necessarily the coolest (Figure S5).

4 | DISCUSSION

Our study provided evidence that stream temperatures during the summer low flow period were generally warmer, but exhibited less diel variation, in Coast Range headwater streams compared to Cascade Range streams in Northern California. Specifically, mean daily stream temperatures were ~4.7°C warmer in the Coast Range despite greater riparian canopy closure and air temperatures that were ~1.6°C cooler than in the Cascade Range (Table 3). Our observations in the Coast Range catchments, which occurred in the Caspar Creek Experimental Watershed Study, were consistent with stream temperature measurements collected over 8 years, between 1965–1990, from catchments in the same region (Cafferata, 1990). For example, while we observed summer maximum stream temperatures of 12.5°C

and diel variation of 0.9°C, Cafferata (1990) reported summer maximums of ~13.3–15.6°C and diurnal fluctuations of 0.8°C. Cool summer stream temperatures in Coast Range streams have previously been attributed to the insulating effect of the dense riparian canopy, high humidity, and coastal fog due to the proximity to the Pacific Ocean (Cafferata & Reid, 2013; Lewis et al., 2000; Moore, Spittlehouse, & Story, 2005; Moore, Sutherland, et al., 2005). In particular, a dense forest canopy cover, as observed in the Coast Range (85%), has been found to limit energy exchange across the stream-air interface and thus, act as a first order control on the magnitude of stream temperature and thermal sensitivity (Chang & Psaris, 2013; Simmons et al., 2015; Winfree et al., 2018).

Our measurements of the longitudinal variability in stream temperature also indicated that the streams in both the Coast Range and the Cascade Range exhibited complex thermal profiles (Fullerton et al., 2015). The longitudinal stream temperature profiles across all our study streams included multiple discontinuities, with sections of increasing and decreasing temperatures (Figure 4). However, there was greater longitudinal thermal heterogeneity in the Cascade Range streams, warming slightly moving downstream but cooling dramatically (2.0 to 7.0°C drops) at discrete locations. Overall, this resulted in cooler average stream temperatures in the Cascade Range streams, despite warmer air temperatures and a less dense riparian canopy in this region. Similar discontinuities in stream temperature have previously been related to discrete groundwater discharge locations, which can thermally buffer streams against daily and seasonal temperature fluctuations (Snyder et al., 2015; Webb et al., 2008). Indeed, the Cascade Range streams were underlain by highly fractured basalt bedrock, which is known to have high water holding capacity and high permeability, resulting in the majority of precipitation draining to groundwater and reemerging as cool springs (Jefferson et al., 2006; Tague et al., 2007; Tague et al., 2008). Reduced diel stream temperature variation in the Cascade Range streams may also have been suggestive of the presence of concentrated groundwater discharge (Harrington et al., 2017; Surfleet & Louen, 2018). However, snow dominated precipitation in the Cascades may confer additional cooling effects on stream water that are not evident in the rain dominated Coast Range. Previous studies in the Pacific Northwest and in the Alaskan boreal forest have illustrated dampening of stream temperatures in snowmelt dominated catchments relative to rain dominated catchments due to greater advective fluxes of cool water, which can dominate over surface energy exchanges (Leach & Moore, 2014; Lisi et al., 2015).

This complexity in the thermal regimes of streams within a region, illustrates the need for additional studies to quantify stream temperature in space and time (Leach & Moore, 2011; Selker et al., 2006). In particular, there remains a critical need to understand the relative importance of discrete groundwater discharge locations and warmer stream segments, which each can provide unique and important ecological values (Armstrong et al., 2021; Torgersen et al., 1999). For example, in the Shasta River, a tributary to the Klamath in Northern California, the thermal influence of spring discharge persisted downstream for 23 km suggesting that understanding similar patterns was critical for managing cold-water fish habitat (Nichols et al., 2014). Downstream cooling has been observed in other spring dominated systems (Bladon et al., 2018; Leach & Moore, 2011; Surfleet & Louen, 2018), and has often been associated with the location of fractures or faults along underlying bedrock. Depending on the volume of groundwater discharge at these locations, stream temperatures may be modified for long distances downstream, with potentially important implications for aquatic habitat.

While the thermal profiles in the Coast Range streams were also complex, the downstream temperature variability was less dramatic. The comparatively thin, friable soils in the Coast Range likely contributed to summer baseflow from spatially continuous shallow subsurface sources or perched areas of saturated soil on most of the streams (Keppeler & Brown, 1998), rather than discrete discharge from deep aquifers. Lateral inflow from a shallow layer at the base of the soil profile has previously been observed as the primary source of baseflow and a dominant control on stream temperature in a Coast Range watershed in the PNW (Moore, Spittlehouse, & Story, 2005; Moore, Sutherland, et al., 2005). Additionally, the step-pool geomorphology in the Coast Range streams may have contributed to hyporheic downwelling or sub-surface inter-gravel flow, which can contribute to greater thermal stability (Kasahara & Wondzell, 2003; Peterson & Sickbert, 2006). Moreover, forest vegetation influences the amount of solar radiation reaching the stream and affecting stream temperature (Roon et al., 2021; Swartz et al., 2020). Thus, the dense canopy in the Coast Range sites could have limited stream warming by solar radiation, further precluding observations of groundwater discharge on those streams by contributing to longitudinal stability in the thermal regime.

Our results also highlighted the spatial variability in stream thermal sensitivity between the Coast Range and Cascade Range streams. Given the regional differences in climate and forest cover, we expected the slope of the relation between air temperature on stream temperature (i.e., thermal sensitivity) to be greater in the Cascade Range streams. However, streams were less thermally sensitive in the Cascade Range by 0.039–0.171°C °C^{-1} compared to the Coast Range streams. Indeed, many stream segments along the Cascade Range streams were insensitive, despite large diel variability in air temperature. These low thermal sensitivities are indicative of a decoupling of stream temperature from atmospheric energy exchange that may have been due to the concentrated groundwater discharge of cold snowmelt from deep aquifers. Site level thermal sensitivity values in Cascade Range streams revealed that values less than 0.2°C °C^{-1} generally corresponded to locations with the coolest and least variable stream temperatures and likely, this threshold separated groundwater dominated versus surface flow dominated portions of the streams (Kelleher et al., 2012; O'Driscoll & DeWalle, 2006).

The effects of groundwater discharge on stream thermal sensitivity has previously been observed in a comparison between spring dominated streams draining resistant volcanic lithology in the high Cascades and shallow sub-surface flow dominated streams draining less resistant lithology in the mid-Cascades of Oregon (Tague et al., 2007). In that study, groundwater discharge in the high

TABLE 6 Results from our study and other studies that have quantified stream thermal sensitivity to air temperature at a range of spatial scales

Thermal sensitivity range (°C °C^{-1})	Location	Temporal resolution	References
0.04–0.77	8 streams in Northern California, US	Daily	Present study
0.19–0.67	12 sites in a Pennsylvania watershed	Weekly	O'Driscoll & DeWalle, 2006
0.39–0.61	6 sites across northern latitudes of the US	Daily	Simmons et al., 2015
0.35–1.09	43 streams internationally	Daily, Weekly	Morrill et al., 2005
0.20–0.65	80 boreal streams in SW Alaska	Daily	Lisi et al., 2015
0.02–0.93	57 sites across Pennsylvania	Daily, Weekly	Kelleher et al., 2012
0.10–0.82	78 sites in Shenandoah National Park, Virginia, US	Daily	Snyder et al., 2015
0.10–0.81	74 sites in the Columbia River Basin, US	Daily, Weekly	Chang & Psaris, 2013
0.13–1.25	157 sites across US, Air Temp >0°C	Weekly, Monthly	Segura et al., 2015
0.20–1.14	104 sites across US PNW	Weekly	Mayer, 2012
0.02–1.09	43 sites across the Oregon Cascades	Daily	Tague et al., 2007
0.13–0.79	46 sites across Maryland, US	Daily	Hilderbrand et al., 2014
0.01–0.58	43 coastal streams in SW Alaska	Daily	Winfree et al., 2018
0.49–1.08	61 sites across the Southeast US	Monthly	Caldwell et al., 2015

Cascades resulted in less thermally sensitive streams compared to the lower elevation shallow sub-surface flow systems. Headwater streams draining volcanic lithology and deep soils typically have a large proportion of summer baseflow generated from groundwater (Segura et al., 2019) that is derived from cold snowmelt water or heavy rains (Tague et al., 2008). These inputs can dampen thermal sensitivity at discrete groundwater discharge locations, where the response to atmospheric warming may lag or mute air temperature signals (Briggs, Johnson, et al., 2018; Briggs, Lane, et al., 2018). We posit that we observed similar processes in our study, whereby the groundwater discharge of cold snowmelt may have dampened stream temperatures in the Cascade Range streams. In comparison, the dense vegetation around the Coast Range streams likely limited stream warming from solar radiation, resulting in longitudinally stable stream temperatures and a reduced ability to detect locations of groundwater discharge.

There have been many previous studies that have assessed stream thermal sensitivity; however, the majority have occurred at a regional or larger scale across multiple river basins, rather than in headwater streams (Table 6). Many of these studies have found strong relationships between stream temperatures and air temperatures (Hilderbrand et al., 2014; Segura et al., 2015; Snyder et al., 2015), indicative of the importance of stream-atmosphere energy exchanges for stream temperature. However, the importance of atmospheric energy exchange may be governed by other factors. For instance, Lisi et al. (2015) observed thermal sensitivity 5–8-times greater in low elevation, low gradient, rain dominated streams compared to high elevation, steep, snowmelt dominated streams due mainly to differences in slope and snowmelt contributions. Several other studies have illustrated low thermal sensitivity in groundwater dominated systems (Kanno et al., 2014; Kelleher et al., 2012; Segura et al., 2015; Tague et al., 2007). Spatially variable groundwater inputs can create strong longitudinal variability in thermal sensitivity (Kanno et al., 2014; O'Driscoll & DeWalle, 2006; Trumbo et al., 2014). In the present study, it is likely that a combination of site-level differences in groundwater contributions, precipitation regime (snow vs. rain), riparian vegetation density, and discharge all exerted an influence on stream temperature, resulting in substantial spatial variability, which requires additional research.

5 | CONCLUSIONS

We compared the longitudinal thermal regimes and thermal sensitivity of eight headwater streams across two distinct regions of Northern California. We used thermal sensitivity as a proxy for stream-atmosphere energy exchanges to facilitate comparisons of potentially different drivers of stream temperature in the two study regions. In general, stream and air temperatures were less coupled in streams underlain by volcanic lithology compared to streams underlain by sedimentary lithology. We posit that the lower thermal sensitivity in the Cascade Range streams may be indicative of cool groundwater discharge, which is known to reduce the coupling of atmospheric energy inputs and stream temperature. Interestingly, we also observed less variability in longitudinal stream temperatures in the Coast Range streams—underlain by sedimentary lithology—despite a slight warming in the downstream direction. This was likely due to greater sensitivity of the shallower subsurface sources of water in the Coast Range streams to non-advective energy exchange through net radiation or latent and sensible heat transfer from the atmosphere. Our study revealed the complexities in thermal regimes in headwater streams and the potential importance of lithology. Improved understanding of the dominant controls on thermal regimes of small headwater streams will become increasingly critical in the future. This knowledge is necessary to improve projections of aquatic habitat resiliency or vulnerability to

pressures from climate change or shifting disturbance regimes, where land management decisions may become increasingly complex. As such, future research should continue to quantify the comparative roles of streamflow, groundwater, and streamside vegetation on fine-scale temperature dynamics and aquatic habitat viability in headwater streams across diverse regions. Additional research is also needed on downstream thermal propagation from spring dominated and shallow subsurface dominated headwater catchments.

ACKNOWLEDGEMENTS

We thank Drew Coe and Elizabeth Keppeler for facilitating development of the research ideas and selection of field site. We also thank Johnathan Tenny, Noah Kanzig, Isaac Friday, Adam Pate, Jonah Nicholas, Samuel Zamudio, and Katie Wampler for their assistance installing field equipment and collecting data. We thank the editors and two anonymous reviewers for their thoughtful suggestions. This research was funded by the California Board of Forestry and Fire Protection Effectiveness Monitoring Committee, grant numbers 8CA03650 and 9CA04452.

DATA AVAILABILITY STATEMENT

The data that support the findings of this study are available from the corresponding author upon reasonable request.

ORCID

Austin D. Wissler https://orcid.org/0000-0001-8368-0053
Catalina Segura https://orcid.org/0000-0002-0924-1172
Kevin D. Bladon https://orcid.org/0000-0002-4182-6883

REFERENCES

Amatya, D., Campbell, J., Wohlgemuth, P., Elder, K., Sebestyen, S., Johnson, S., Keppeler, E., Adams, M. B., Caldwell, P., & Misra, D. (2016). Hydrological processes of reference watersheds in experimental forests, USA. In D. M. Amatya, T. M. Williams, L. Bren, & C. de Jong (Eds.), *Forest hydrology: Processes, management, and applications*. U.S. Forest Service, Southern Research Station.

Arismendi, I., Dunham, J. B., Heck, M. P., Schultz, L. D., & Hockman-Wert, D. (2017). A statistical method to predict flow permanence in dryland streams from time series of stream temperature. *Water*, *9*, 13. https://doi.org/10.3390/w9120946

Arismendi, I., Safeeq, M., Dunham, J. B., & Johnson, S. L. (2014). Can air temperature be used to project influences of climate change on stream temperature? *Environmental Research Letters*, *9*, 12. https://doi.org/10.1088/1748-9326/9/8/084015

Arismendi, I., Safeeq, M., Johnson, S. L., Dunham, J. B., & Haggerty, R. (2013). Increasing synchrony of high temperature and low flow in western north American streams: Double trouble for Coldwater biota? *Hydrobiologia*, *712*, 61–70. https://doi.org/10.1007/s10750-012-1327-2

Armstrong, J. B., Fullerton, A. H., Jordan, C. E., Ebersole, J. L., Bellmore, J. R., Arismendi, I., Penaluna, B. E., & Reeves, G. H. (2021). The importance of warm habitat to the growth regime of cold-water fishes. *Nature Climate Change*, *11*, 354–361. https://doi.org/10.1038/s41558-021-00994-y

Arscott, D. B., Tockner, K., & Ward, J. V. (2001). Thermal heterogeneity along a braided floodplain river (Tagliamento River, northeastern Italy). *Canadian Journal of Fisheries and Aquatic Sciences*, *58*, 2359–2373. https://doi.org/10.1139/cjfas-58-12-2359

Bateman, D. S., Chelgren, N. D., Gresswell, R. E., Dunham, J. B., Hockman-Wert, D. P., Leer, D. W., & Bladon, K. D. (2021). Fish response to successive clearcuts in a second-growth forest from the central Coast Range of Oregon. *Forest Ecology and Management*, *496*, 119447. https://doi.org/10.1016/j.foreco.2021.119447

Benjamin, J. R., Connolly, P. J., Romine, J. G., & Perry, R. W. (2013). Potential effects of changes in temperature and food resources on life history trajectories of juvenile *Oncorhynchus mykiss*. *Transactions of the American Fisheries Society*, *142*, 208–220. https://doi.org/10.1080/00028487.2012.728162

Bernhardt, E. S., Heffernan, J. B., Grimm, N. B., Stanley, E. H., Harvey, J. W., Arroita, M., Appling, A. P., Cohen, M. J., McDowell, W. H., Hall, R. O., Read, J. S., Roberts, B. J., Stets, E. G., & Yackulic, C. B. (2018). The metabolic regimes of flowing waters. *Limnology and Oceanography*, *63*, S99–S118. https://doi.org/10.1002/lno.10726

Bladon, K. D., Cook, N. A., Light, J. T., & Segura, C. (2016). A catchment-scale assessment of stream temperature response to contemporary forest harvesting in the Oregon Coast Range. *Forest Ecology & Management*, *379*, 153–164. https://doi.org/10.1016/j.foreco.2016.08.021

Bladon, K. D., Segura, C., Cook, N. A., Bywater-Reyes, S., & Reiter, M. (2018). A multi-catchment analysis of headwater and downstream temperature effects from contemporary forest harvesting. *Hydrological Processes*, *32*, 293–304. https://doi.org/10.1002/hyp.11415

Brewitt, K. S., Danner, E. M., & Moore, J. W. (2017). Hot eats and cool creeks: Juvenile Pacific salmonids use mainstem prey while in thermal refuges. *Canadian Journal of Fisheries and Aquatic Sciences*, *74*, 1588–1602. https://doi.org/10.1139/cjfas-2016-0395

Briggs, M. A., Dawson, C. B., Holmquist-Johnson, C. L., Williams, K. H., & Lane, J. W. (2019). Efficient hydrogeological characterization of remote stream corridors using drones. *Hydrological Processes*, *33*, 316–319. https://doi.org/10.1002/hyp.13332

Briggs, M. A., Johnson, Z. C., Snyder, C. D., Hitt, N. P., Kurylyk, B. L., Lautz, L., Irvine, D. J., Hurley, S. T., & Lane, J. W. (2018). Inferring watershed hydraulics and cold-water habitat persistence using multi-year air and stream temperature signals. *Science of the Total Environment*, *636*, 1117–1127. https://doi.org/10.1016/j.scitotenv.2018.04.344

Briggs, M. A., Lane, J. W., Snyder, C. D., White, E. A., Johnson, Z. C., Nelms, D. L., & Hitt, N. P. (2018). Shallow bedrock limits groundwater seepage-based headwater climate refugia. *Limnologica*, *68*, 142–156. https://doi.org/10.1016/j.limno.2017.02.005

Brown, L. E., & Hannah, D. M. (2008). Spatial heterogeneity of water temperature across an alpine river basin. *Hydrological Processes*, *22*, 954–967. https://doi.org/10.1002/hyp.6982

Cafferata, P. H. (1990). *Temperature regimes of small streams along the Mendocino coast* (pp. 1–4). Jackson Demonstration State Forest Newsletter, California Department of Forestry.

Cafferata, P. H., & Reid, L. M. (2013). *Applications of long-term watershed research to forest management in California: 50 years of learning from the Caspar Creek watershed study* (p. 114). Department of Forestry & Fire Protection.

Caissie, D. (2006). The thermal regime of rivers: A review. *Freshwater Biology*, *51*, 1389–1406. https://doi.org/10.1111/j.1365-2427.2006.01597.x

CAL FIRE (2008). In R. M (Ed.), *LaTour demonstration state forest management plan* (p. 94). California Department of Forestry and Fire Protection.

Caldwell, P., Segura, C., Laird, S. G., Sun, G., McNulty, S. G., Sandercock, M., Boggs, J., & Vose, J. M. (2015). Short-term stream water temperature observations permit rapid assessment of potential climate change impacts. *Hydrological Processes*, *29*, 2196–2211. https://doi.org/10.1002/hyp.10358

Campbell, J. L., Rustad, L. E., Porter, J. H., Taylor, J. R., Dereszynski, E. W., Shanley, J. B., Gries, C., Henshaw, D. L., Martin, M. E., Sheldon, W. M., & Boose, E. R. (2013). Quantity is nothing without quality: Automated QA/QC for streaming environmental sensor data. *Bioscience*, *63*, 574–585. https://doi.org/10.1525/bio.2013.63.7.10

Chang, H. J., & Psaris, M. (2013). Local landscape predictors of maximum stream temperature and thermal sensitivity in the Columbia River basin, USA. *Science of the Total Environment*, *461*, 587–600. https://doi.org/10.1016/j.scitotenv.2013.05.033

Dallas, H. F., & Ross-Gillespie, V. (2015). Sublethal effects of temperature on freshwater organisms, with special reference to aquatic insects. *Water SA*, *41*, 712–726. https://doi.org/10.4314/wsa.v41i5.15

Danehy, R. J., Colson, C. G., & Duke, S. D. (2010). Winter longitudinal thermal regime in four mountain streams. *Northwest Science*, *84*, 151–158. https://doi.org/10.3955/046.084.0204

Dent, L., Vick, D., Abraham, K., Schoenholtz, S., & Johnson, S. (2008). Summer temperature patterns in headwater streams of the Oregon Coast Range. *Journal of the American Water Resources Association*, *44*, 803–813. https://doi.org/10.1111/j.1752-1688.2008.00204.x

Dugdale, S. J., Bergeron, N. E., & St-Hilaire, A. (2015). Spatial distribution of thermal refuges analysed in relation to riverscape hydromorphology using airborne thermal infrared imagery. *Remote Sensing of Environment*, *160*, 43–55. https://doi.org/10.1016/j.rse.2014.12.021

Eaton, J. G., & Scheller, R. M. (1996). Effects of climate warming on fish thermal habitat in streams of the United States. *Limnology and Oceanography*, *41*, 1109–1115. https://doi.org/10.4319/lo.1996.41.5.1109

Ebersole, J. L., Wigington, P. J., Leibowitz, S. G., Comeleo, R. L., & Van Sickle, J. (2015). Predicting the occurrence of cold-water patches at intermittent and ephemeral tributary confluences with warm rivers. *Freshwater Science*, *34*, 111–124. https://doi.org/10.1086/678127

Fullerton, A. H., Torgersen, C. E., Lawler, J. J., Faux, R. N., Steel, E. A., Beechie, T. J., Ebersole, J. L., & Leibowitz, S. G. (2015). Rethinking the longitudinal stream temperature paradigm: Region-wide comparison of thermal infrared imagery reveals unexpected complexity of river temperatures. *Hydrological Processes*, *29*, 4719–4737. https://doi.org/10.1002/hyp.10506

Fullerton, A. H., Torgersen, C. E., Lawler, J. J., Steel, E. A., Ebersole, J. L., & Lee, S. Y. (2018). Longitudinal thermal heterogeneity in rivers and refugia for Coldwater species: Effects of scale and climate change. *Aquatic Sciences*, *80*, 15. https://doi.org/10.1007/s00027-017-0557-9

Gendaszek, A. S., Dunham, J. B., Torgersen, C. E., Hockman-Wert, D. P., Heck, M. P., Thorson, J., Mintz, J., & Allai, T. (2020). Land-cover and climatic controls on water temperature, flow permanence, and fragmentation of Great Basin stream networks. *Water*, *12*, 1962. https://doi.org/10.3390/w12071962

Gomi, T., Moore, R. D., & Dhakal, A. S. (2006). Headwater stream temperature response to clear-cut harvesting with different riparian treatments, coastal British Columbia, Canada. *Water Resources Research*, *42*, W08437. https://doi.org/10.1029/2005WR004162

Griebler, C., & Avramov, M. (2015). Groundwater ecosystem services: A review. *Freshwater Science*, *34*, 355–367. https://doi.org/10.1086/679903

Groom, J. D., Johnson, S. L., Seeds, J. D., & Ice, G. G. (2017). Evaluating links between forest harvest and stream temperature threshold exceedances: The value of spatial and temporal data. *Journal of the American Water Resources Association*, *53*(4), 761–773. https://doi.org/10.1111/1752-1688.12529

Gu, C. H., Anderson, W. P., Colby, J. D., & Coffey, C. L. (2015). Air-stream temperature correlation in forested and urban headwater streams in the southern Appalachians. *Hydrological Processes*, *29*, 1110–1118. https://doi.org/10.1002/hyp.10225

Hale, V. C., & McDonnell, J. J. (2016). Effect of bedrock permeability on stream base flow mean transit time scaling relations: 1. A multiscale catchment intercomparison. *Water Resources Research*, *52*, 1358–1374. https://doi.org/10.1002/2014WR016124

Harrington, J. S., Hayashi, M., & Kurylyk, B. L. (2017). Influence of a rock glacier spring on the stream energy budget and cold-water refuge in an alpine stream. *Hydrological Processes*, *31*, 4719–4733. https://doi.org/10.1002/hyp.11391

Hester, E. T., & Doyle, M. W. (2011). Human impacts to river temperature and their effects on biological processes: A quantitative synthesis. *Journal of the American Water Resources Association*, *47*, 571–587. https://doi.org/10.1111/j.1752-1688.2011.00525.x

Hilderbrand, R. H., Kashiwagi, M. T., & Prochaska, A. P. (2014). Regional and local scale modeling of stream temperatures and spatio-temporal variation in thermal sensitivities. *Environmental Management*, *54*, 14–22. https://doi.org/10.1007/s00267-014-0272-4

Hofmeister, K. L., Cianfrani, C. M., & Hession, W. C. (2015). Complexities in the stream temperature regime of a small mixed-use watershed, Blacksburg, VA. *Ecological Engineering*, *78*, 101–111. https://doi.org/10.1016/j.ecoleng.2014.05.019

Jackson, F. L., Fryer, R. J., Hannah, D. M., Millar, C. P., & Malcolm, I. A. (2018). A spatio-temporal statistical model of maximum daily river temperatures to inform the management of Scotland's Atlantic salmon rivers under climate change. *Science of the Total Environment*, *612*, 1543–1558. https://doi.org/10.1016/j.scitotenv.2017.09.010

Jaeger, K. L., Montgomery, D. R., & Bolton, S. M. (2007). Channel and perennial flow initiation in headwater streams: Management implications of variability in source-area size. *Environmental Management*, *40*, 775–786. https://doi.org/10.1007/s00267-005-0311-2

Jager, H. I., Long, J. W., Malison, R. L., Murphy, B. P., Rust, A., Silva, L. G. M., Sollmann, R., Steel, Z. L., Bowen, M. D., Dunham, J. B., Ebersole, J. L., & Flitcroft, R. L. (2021). Resilience of terrestrial and aquatic fauna to historical and future wildfire regimes in western North America. *Ecology and Evolution*, *11*, 12259–12284. https://doi.org/10.1002/ece3.8026

Janisch, J. E., Wondzell, S. M., & Ehinger, W. J. (2012). Headwater stream temperature: Interpreting response after logging, with and without riparian buffers, Washington, USA. *Forest Ecology and Management*, *270*, 302–313. https://doi.org/10.1016/j.foreco.2011.12.035

Jefferson, A., Grant, G., & Rose, T. (2006). Influence of volcanic history on groundwater patterns on the west slope of the Oregon High Cascades. *Water Resources Research*, *42*, 15. https://doi.org/10.1029/2005wr004812

Johnson, M. F., Wilby, R. L., & Toone, J. A. (2014). Inferring air- water temperature relationships from river and catchment properties. *Hydrological Processes*, *28*, 2912–2928. https://doi.org/10.1002/hyp.9842

Johnson, S. L. (2003). Stream temperature: Scaling of observations and issues for modelling. *Hydrological Processes*, *17*, 497–499. https://doi.org/10.1002/hyp.5091

Kanno, Y., Vokoun, J. C., & Letcher, B. H. (2014). Paired stream-air temperature measurements reveal fine-scale thermal heterogeneity within headwater brook trout stream networks. *River Research and Applications*, *30*, 745–755. https://doi.org/10.1002/rra.2677

Kasahara, T., & Wondzell, S. M. (2003). Geomorphic controls on hyporheic exchange flow in mountain streams. *Water Resources Research*, *39*, SBH 3-1–SBH 3-14. https://doi.org/10.1029/2002wr001386

Kelleher, C., Wagener, T., Gooseff, M., McGlynn, B., McGuire, K., & Marshall, L. (2012). Investigating controls on the thermal sensitivity of Pennsylvania streams. *Hydrological Processes*, *26*, 771–785. https://doi.org/10.1002/hyp.8186

Kelson, K. I., & Wells, S. G. (1989). Geologic influences on fluvial hydrology and bedload transport in small mountainous watersheds, northern New Mexico, USA. *Earth Surface Processes and Landforms*, *14*, 671–690. https://doi.org/10.1002/esp.3290140803

Keppeler, E. T., & Brown, D. (1998). Subsurface drainage processes and management impacts. In R. R. Ziemer (Ed.), *Proceedings of the Conference on Coastal Watersheds: The Caspar Creek Story* (pp. 25–34). U.S. Department of Agriculture.

Keppeler, E. T., Ziemer, R. R., & Cafferata, P. H. (1994). In R. A. Marston & V. R. Hasfurther (Eds.), *Changes in soil moisture and pore pressure after harvesting a forested hillslope in northern California* (pp. 205–214). American Water Resources Association.

Kurylyk, B. L., MacQuarrie, K. T. B., Caissie, D., & McKenzie, J. M. (2015). Shallow groundwater thermal sensitivity to climate change and land cover disturbances: Derivation of analytical expressions and implications for stream temperature modeling. *Hydrology and Earth System Sciences*, *19*, 2469–2489. https://doi.org/10.5194/hess-19-2469-2015

Larsen, L. G., & Woelfle-Erskine, C. (2018). Groundwater is key to salmonid persistence and recruitment in intermittent Mediterranean-climate streams. *Water Resources Research*, *54*, 8909–8930. https://doi.org/10.1029/2018wr023324

Larson, S. L., Larson, L. L., & Larson, P. A. (2002). Perspectives on water flow and the interpretation of FLIR images. *Journal of Range Management*, *55*, 106–111. https://doi.org/10.2307/4003344

Leach, J. A., & Moore, R. D. (2011). Stream temperature dynamics in two hydrogeomorphically distinct reaches. *Hydrological Processes*, *25*, 679–690. https://doi.org/10.1002/hyp.7854

Leach, J. A., & Moore, R. D. (2014). Winter stream temperature in the rain-on-snow zone of the Pacific Northwest: Influences of hillslope runoff and transient snow cover. *Hydrology and Earth System Sciences*, *18*, 819–838. https://doi.org/10.5194/hess-18-819-2014

Leach, J. A., & Moore, R. D. (2019). Empirical stream thermal sensitivities may underestimate stream temperature response to climate warming. *Water Resources Research*, *55*, 5453–5467. https://doi.org/10.1029/2018wr024236

LEMMA (2020). Landsat-based maps of forest structure and composition for Washington, Oregon, and California. Landscape Ecology, Modeling, Mapping, and Analysis (http://lemma.forestry.oregonstate.edu/data/structure-maps). Oregon State University, Corvallis, OR.

Lewis, T. E., Lamphear, D. W., McCanne, D. R., Webb, A. S., Krieter, J. P., & Conroy, W. D. (2000). *Regional assessment of stream temperatures across northern California and their relationship to various landscape-level and site-specific attributes* (p. 420). Humboldt State University Foundation.

Lisi, P. J., Schindler, D. E., Cline, T. J., Scheuerell, M. D., & Walsh, P. B. (2015). Watershed geomorphology and snowmelt control stream thermal sensitivity to air temperature. *Geophysical Research Letters*, *42*, 3380–3388. https://doi.org/10.1002/2015gl064083

Loperfido, J. V., Just, C. L., & Schnoor, J. L. (2009). High-frequency diel dissolved oxygen stream data modeled for variable temperature and scale. *Journal of Environmental Engineering*, *135*, 1250–1256. https://doi.org/10.1061/(asce)ee.1943-7870.0000102

Macdonald, G. A. (1963). *Geology of the Manzanita Lake quadrangle*. California.

Mayer, T. D. (2012). Controls of summer stream temperature in the Pacific Northwest. *Journal of Hydrology*, *475*, 323–335. https://doi.org/10.1016/j.jhydrol.2012.10.012

McCullough, D. A., Bartholow, J. M., Jager, H. I., Beschta, R. L., Cheslak, E. F., Deas, M. L., Ebersole, J. L., Foott, J. S., Johnson, S. L., Marine, K. R., Mesa, M. G., Petersen, J. H., Souchon, Y., Tiffan, K. F., & Wurtsbaugh, W. A. (2009). Research in thermal biology: Burning questions for Coldwater stream fishes. *Reviews in Fisheries Science*, *17*, 90–115. https://doi.org/10.1080/10641260802590152

McDonald, S. R. (1995). *LaTour demonstration state forest sustained yield plan* (p. 246). California Department of Forestry and Fire Protection.

Mohseni, O., & Stefan, H. G. (1999). Stream temperature air temperature relationship: A physical interpretation. *Journal of Hydrology*, *218*, 128–141. https://doi.org/10.1016/s0022-1694(99)00034-7

Montgomery, D. R., & Buffington, J. M. (1997). Channel-reach morphology in mountain drainage basins. *Geological Society of America Bulletin*, *109*, 596–611. https://doi.org/10.1130/0016-7606(1997)109<0596:Crmimd>2.3.Co;2

Moore, R. D., Spittlehouse, D. L., & Story, A. (2005). Riparian microclimate and stream temperature response to forest harvesting: A review. *Journal of the American Water Resources Association*, *41*, 813–834. https://doi.org/10.1111/j.1752-1688.2005.tb04465.x

Moore, R. D., Sutherland, P., Gomi, T., & Dhakal, A. (2005). Thermal regime of a headwater stream within a clear-cut, coastal British Columbia, Canada. *Hydrological Processes*, *19*, 2591–2608. https://doi.org/10.1002/hyp.5733

Morin, A., Lamoureux, W., & Busnarda, J. (1999). Empirical models predicting primary productivity from chlorophyll a and water temperature for stream periphyton and lake and ocean phytoplankton. *Journal of the North American Benthological Society*, *18*, 299–307. https://doi.org/10.2307/1468446

Morrice, J. A., Valett, H. M., Dahm, C. N., & Campana, M. E. (1997). Alluvial characteristics, groundwater-surface water exchange and hydrological retention in headwater streams. *Hydrological Processes*, *11*, 253–267. https://doi.org/10.1002/(sici)1099-1085(19970315)11:3<253::Aid-hyp439>3.0.Co;2-j

Morrill, J. C., Bales, R. C., & Conklin, M. H. (2005). Estimating stream temperature from air temperature: Implications for future water quality. *Journal of Environmental Engineering-ASCE*, *131*, 139–146. https://doi.org/10.1061/(asce)0733-9372(2005)131:1(139)

Neres-Lima, V., Machado-Silva, F., Baptista, D. F., Oliveira, R. B. S., Andrade, P. M., Oliveira, A. F., Sasada-Sato, C. Y., Silva, E. F., Feijo-Lima, R., Angelini, R., Camargo, P. B., & Moulton, T. P. (2017). Allochthonous and autochthonous carbon flows in food webs of tropical forest streams. *Freshwater Biology*, *62*, 1012–1023. https://doi.org/10.1111/fwb.12921

Nichols, A. L., Willis, A. D., Jeffres, C. A., & Deas, M. L. (2014). Water temperature patterns below large groundwater springs: Management implications for coho salmon in the Shasta River, California. *River Research and Applications*, *30*, 442–455. https://doi.org/10.1002/rra.2655

NRCS. (2020). *Snow telemetry (SNOTEL) and snow course data and products*. Natural Resources Conservation Service (NRCS) and National Water and Climate Center.

O'Driscoll, M. A., & DeWalle, D. R. (2006). Stream-air temperature relations to classify stream-ground water interactions. *Journal of Hydrology*, *329*, 140–153. https://doi.org/10.1016/j.jhydrol.2006.02.010

O'Sullivan, A. M., Devito, K. J., & Curry, R. A. (2019). The influence of landscape characteristics on the spatial variability of river temperatures. *Catena*, *177*, 70–83. https://doi.org/10.1016/j.catena.2019.02.006

Ozaki, N., Fukushima, T., Harasawa, H., Kojiri, T., Kawashima, K., & Ono, M. (2003). Statistical analyses on the effects of air temperature fluctuations on river water qualities. *Hydrological Processes*, *17*, 2837–2853. https://doi.org/10.1002/hyp.1437

Pate, A. A., Segura, C., & Bladon, K. D. (2020). Streamflow permanence in headwater streams across four geomorphic provinces in Northern California. *Hydrological Processes*, *34*, 4487–4504. https://doi.org/10.1002/hyp.13889

Peterson, E. W., & Sickbert, T. B. (2006). Stream water bypass through a meander neck, laterally extending the hyporheic zone. *Hydrogeology Journal*, *14*, 1443–1451. https://doi.org/10.1007/s10040-006-0050-3

Ploum, S. W., Leach, J. A., Kuglerova, L., & Laudon, H. (2018). Thermal detection of discrete riparian inflow points (DRIPs) during contrasting hydrological events. *Hydrological Processes*, *32*, 3049–3050. https://doi.org/10.1002/hyp.13184

PRISM Climate Group. (2020). *PRISM gridded climate data*. Oregon State University.

R Core Team. (2020). *R: A language and environment for statistical computing*. R Foundation for Statistical Computing.

Roon, D. A., Dunham, J. B., & Groom, J. D. (2021). Shade, light, and stream temperature responses to riparian thinning in second growth redwood

forests of northern California. *PLoS One*, *16*, e0246822. https://doi.org/10.1371/journal.pone.0246822

Segura, C., Caldwell, P., Sun, G., McNulty, S., & Zhang, Y. (2015). A model to predict stream water temperature across the conterminous USA. *Hydrological Processes*, *29*, 2178–2195. https://doi.org/10.1002/hyp.10357

Segura, C., Noone, D., Warren, D., Jones, J. A., Tenny, J., & Ganio, L. M. (2019). Climate, landforms, and geology affect baseflow sources in a mountain catchment. *Water Resources Research*, *55*, 5238–5254. https://doi.org/10.1029/2018wr023551

Selker, J., van de Giesen, N., Westhoff, M., Luxemburg, W., & Parlange, M. B. (2006). Fiber optics opens window on stream dynamics. *Geophysical Research Letters*, *33*, 4. https://doi.org/10.1029/2006gl027979

Simmons, J. A., Anderson, M., Dress, W., Hanna, C., Hornbach, D. J., Janmaat, A., Kuserk, F., March, J. G., Murray, T., Niedzwiecki, J., Panvini, D., Pohlad, B., Thomas, C., & Vasseur, L. (2015). A comparison of the temperature regime of short stream segments under forested and non-forested riparian zones at eleven sites across North America. *River Research and Applications*, *31*, 964–974. https://doi.org/10.1002/rra.2796

Sloat, M. R., & Osterback, A. M. K. (2013). Maximum stream temperature and the occurrence, abundance, and behavior of steelhead trout (*Oncorhynchus mykiss*) in a southern California stream. *Canadian Journal of Fisheries and Aquatic Sciences*, *70*, 64–73. https://doi.org/10.1139/cjfas-2012-0228

Snyder, C. D., Hitt, N. P., & Young, J. A. (2015). Accounting for groundwater in stream fish thermal habitat responses to climate change. *Ecological Applications*, *25*, 1397–1419. https://doi.org/10.1890/14-1354.1

Sowder, C., & Steel, E. A. (2012). A note on the collection and cleaning of water temperature data. *Water*, *4*, 597–606. https://doi.org/10.3390/w4030597

Stefan, H. G., & Preudhomme, E. B. (1993). Stream temperature estimation from air-temperature. *Water Resources Bulletin*, *29*, 27–45. https://doi.org/10.1111/j.1752-1688.1993.tb01502.x

Story, A., Moore, R. D., & Macdonald, J. S. (2003). Stream temperatures in two shaded reaches below cutblocks and logging roads: Downstream cooling linked to subsurface hydrology. *Canadian Journal of Forest Research*, *33*, 1383–1396. https://doi.org/10.1139/x03-087

Surfleet, C., & Louen, J. (2018). The influence of hyporheic exchange on water temperatures in a headwater stream. *Water*, *10*, 15. https://doi.org/10.3390/w10111615

Swartz, A., Roon, D., Reiter, M., & Warren, D. (2020). Stream temperature responses to experimental riparian canopy gaps along forested headwaters in western Oregon. *Forest Ecology and Management*, *474*, 118354. https://doi.org/10.1016/j.foreco.2020.118354

Tague, C., Farrell, M., Grant, G., Lewis, S., & Rey, S. (2007). Hydrogeologic controls on summer stream temperatures in the McKenzie River basin, Oregon. *Hydrological Processes*, *21*, 3288–3300. https://doi.org/10.1002/hyp.6538

Tague, C., Grant, G., Farrell, M., Choate, J., & Jefferson, A. (2008). Deep groundwater mediates streamflow response to climate warming in the Oregon Cascades. *Climatic Change*, *86*, 189–210. https://doi.org/10.1007/s10584-007-9294-8

Thomas, C. D., Cameron, A., Green, R. E., Bakkenes, M., Beaumont, L. J., Collingham, Y. C., Erasmus, B. F. N., de Siqueira, M. F., Grainger, A., Hannah, L., Hughes, L., Huntley, B., van Jaarsveld, A. S., Midgley, G. F., Miles, L., Ortega-Huerta, M. A., Peterson, A. T., Phillips, O. L., & Williams, S. E. (2004). Extinction risk from climate change. *Nature (London)*, *427*, 145–148. https://doi.org/10.1038/nature02121

Torgersen, C. E., Price, D. M., Li, H. W., & McIntosh, B. A. (1999). Multiscale thermal refugia and stream habitat associations of chinook salmon in northeastern Oregon. *Ecological Applications*, *9*, 301–319. https://doi.org/10.2307/2641187

Trumbo, B. A., Nislow, K. H., Stallings, J., Hudy, M., Smith, E. P., Kim, D. Y., Wiggins, B., & Dolloff, C. A. (2014). Ranking site vulnerability to increasing temperatures in southern Appalachian brook trout streams in Virginia: An exposure-sensitivity approach. *Transactions of the American Fisheries Society*, *143*, 173–187. https://doi.org/10.1080/00028487.2013.835282

Vannote, R. L., Minshall, G. W., Cummins, K. W., Sedell, J. R., & Cushing, C. E. (1980). The river continuum concept. *Canadian Journal of Fisheries and Aquatic Sciences*, *37*, 130–137. https://doi.org/10.1139/f80-017

Wagner, M. J., Bladon, K. D., Silins, U., Williams, C. H. S., Martens, A. M., Boon, S., MacDonald, R. J., Stone, M., Emelko, M. B., & Anderson, A. (2014). Catchment-scale stream temperature response to land disturbance by wildfire governed by surface-subsurface energy exchange and atmospheric controls. *Journal of Hydrology*, *517*, 328–338. https://doi.org/10.1016/j.jhydrol.2014.05.006

Webb, B. W., Hannah, D. M., Moore, R. D., Brown, L. E., & Nobilis, F. (2008). Recent advances in stream and river temperature research. *Hydrological Processes*, *22*, 902–918. https://doi.org/10.1002/hyp.6994

Welsh, H. H., Hodgson, G. R., Harvey, B. C., & Roche, M. F. (2001). Distribution of juvenile Coho salmon in relation to water temperatures in tributaries of the Mattole River, California. *North American Journal of Fisheries Management*, *21*, 464–470. https://doi.org/10.1577/1548-8675(2001)021<0464:Dojcsi>2.0.Co;2

Westhoff, J. T., & Paukert, C. P. (2014). Climate change simulations predict altered biotic response in a thermally heterogeneous stream system. *PLoS One*, *9*, 15. https://doi.org/10.1371/journal.pone.0111438

Westhoff, M. C., Gooseff, M. N., Bogaard, T. A., & Savenije, H. H. G. (2011). Quantifying hyporheic exchange at high spatial resolution using natural temperature variations along a first-order stream. *Water Resources Research*, *47*, 13. https://doi.org/10.1029/2010wr009767

Winfree, M. M., Hood, E., Stuefer, S. L., Schindler, D. E., Cline, T. J., Arp, C. D., & Pyare, S. (2018). Landcover and geomorphology influence streamwater temperature sensitivity in salmon bearing watersheds in Southeast Alaska. *Environmental Research Letters*, *13*, 10. https://doi.org/10.1088/1748-9326/aac4c0

Xu, C. L., Letcher, B. H., & Nislow, K. H. (2010). Size-dependent survival of brook trout Salvelinus fontinalis in summer: Effects of water temperature and stream flow. *Journal of Fish Biology*, *76*, 2342–2369. https://doi.org/10.1111/j.1095-8649.2010.02619.x

SUPPORTING INFORMATION

Additional supporting information may be found in the online version of the article at the publisher's website.

How to cite this article: Wissler, A. D., Segura, C., & Bladon, K. D. (2022). Comparing headwater stream thermal sensitivity across two distinct regions in Northern California. *Hydrological Processes*, *36*(3), e14517. https://doi.org/10.1002/hyp.14517